Monodisperse Particles

DOI: 10.1002/anie.201002764

Surface-Tension-Induced Synthesis of Complex Particles Using Confined Polymeric Fluids**

*Chang-Hyung Choi, Jinkee Lee, Kisun Yoon, Anubhav Tripathi, Howard A. Stone, David A. Weitz, and Chang-Soo Lee**

Polymeric particles are used in a variety of applications such as systems for controlled chemical release,[1–9] optical materials,[10,11] chromatographic media,[12] and various biological applications.[13–16] The physical and chemical properties of polymeric particles, such as their shape, size, porosity, surface charge, and hydrophilicity or hydrophobicity, influence the particle function and are important for their use in microrheology and for their applications in materials and self-assembly.[17–22] Therefore, a novel methodology for the generation of uniform particles with a large diversity of design morphologies and physicochemical properties would be a promising platform for many advanced applications.

Conventional approaches for the synthesis of polymeric particles with various shapes are self-assembly,[23,24] photolithography,[25–28] stretching or deformation of spherical particles,[29,30] microfluidics,[9,21,22,31–38] and nonwetting template molding.[6,13,39] The synthesis of particles that have complex shapes, however, can not be easily executed because of difficulties in handling various polymers in a controlled way. Most current techniques have been limited to 2D or spherical shapes although the techniques can control the chemical and physical properties of individual particles.

[*] C.-H. Choi,[+] Prof. C.-S. Lee
Department of Chemical Engineering
Chungnam National University
Yuseong-gu, Daejeon 305-764 (South Korea)
E-mail: rhadum@cnu.ac.kr
K. Yoon, Prof. D. A. Weitz
School of Engineering and Applied Sciences
Harvard University, Cambridge, MA 02138 (USA)
Dr. J. Lee,[+] Prof. A. Tripathi
Division of Engineering, Brown University
Providence, RI 02912 (USA)
Prof. H. A. Stone
Department of Mechanical and Aerospace Engineering
Princeton University, Princeton, NJ 08544 (USA)
[+] These authors contributed equally to this work.

[**] This study was supported by the Converging Research Center Program through the National Research Foundation of Korea (NRF) funded by the Ministry of Education, Science and Technology (2009-0082087), the Industrial Source Technology Development Programs (10033093) of the Ministry of Knowledge Economy (MKE) of Korea, a grant from the Korea Health 21 R&D Project, Ministry of Health and Welfare (Project No. A062254), Korea Science and Engineering Foundation (KOSEF) grant funded by the Korean Government (MEST) (MEST No. R01-2008-000-11260-0), the NSF-sponsored Materials Research Science and Engineering Center at Harvard University (DMR-0820484), and the NSF (DMR-0602684).

Supporting information for this article is available on the WWW under http://dx.doi.org/10.1002/anie.201002764.

Each synthetic method possesses unique advantages and limitations. For example, "bottom-up" approaches based on self-assembly mechanisms such as liposome preparation, heterogeneous polymerization, and colloid synthesis are difficult to manipulate to provide reasonable control of both morphology and structure.[23,24] Alternatively, the "top-down" approaches such as photolithography are inherently limited by the availability of materials. In general, photolithography is not compatible with organic materials and leads to the degradation of materials, as this technique typically requires processing techniques such as wet etching with harsh solvents, reactive ion etching with high energy, baking at high temperatures, multiple steps for removal of sacrificial layers, and strong energy deposition.[25–28] Microfluidic platforms allow the generation of spherical and 2D shapes such as disks, plugs, or rods in accordance with microchannel or photomask geometries and flow conditions.[9,21,22,31–38] However, the microfluidic methods also experience technical limitations: Firstly, fast solidification without deformation and sticking on the channel is required, and secondly, the morphologies of particles produced are limited by channel or photomask geometries. Most recently, an advanced approach described as particle replication in nonwetting templates (PRINT) has been developed to fabricate monodisperse particles of varying size and shape.[6,13,39] This technique provides reproducibility and easy processing and can be used with a wide range of materials. However, it is still difficult to make 3D shapes such as spheres, convex or concave particles, and complex janus particles. Therefore, there remains a need for a simple, robust, and high-throughput method of particle fabrication that can provide custom-designed shapes, compositions, sizes, and compartmentalization for 2D and 3D shapes.

Herein, we demonstrate a new method for synthesizing a range of monodisperse particles through surface-tension-induced flow. We provide examples of particles with various shapes such as bullets, cylinders, discs, hemispheres, hearts, twin cylinders, twin donuts, hexagons with open or closed ends, and Janus particles. The complex-shaped particles produced by our approach can be exploited as anisotropic building blocks for fabrication of complex systems. We present two different routes for the generation of uniformly sized polymeric particles with different morphologies such as convex and flat-top shapes (Figure 1). A photocurable solution (polyethylene glycol diacrylate; PEG-DA) and a nonphotocurable wetting solution (*n*-hexadecane) are sequentially loaded into a micromold. The different processes in a loading sequence of the two solutions of P and H (sequences A and B; Figure 1) resulted in formation of different contacting interfaces of *n*-hexadecane/PEG-DA and

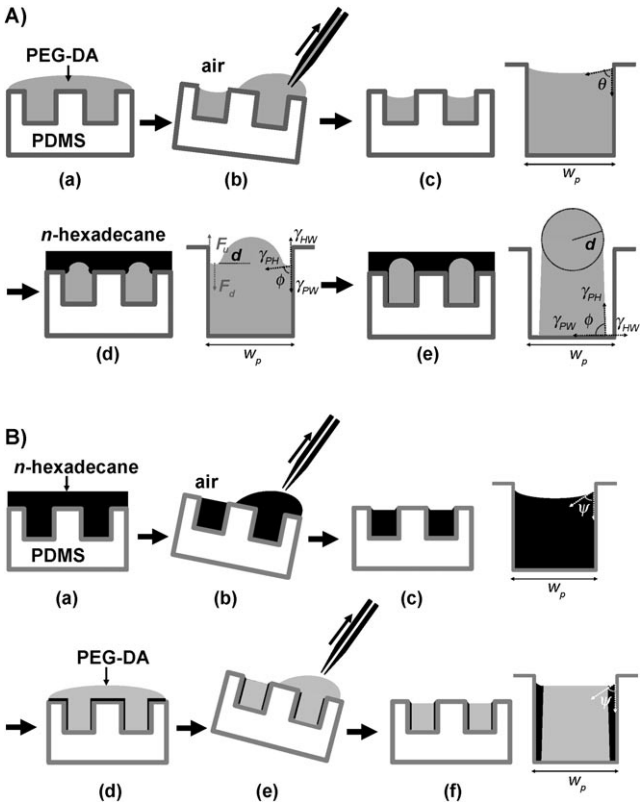

Figure 1. Diagrams of the detailed procedure of sequences A and B for the synthesis of particles with complex shapes. A) Sequence A; a) loading of polymerizing solution (PEG-DA), b) removal of excess PEG-DA solution by tilting, c) generation of an interface between PEG-DA and air, d) pouring wetting solution (*n*-hexadecane) onto the PDMS mold which changes the contact angle; surface tension forces of the wetting fluid along the PDMS wall act because of the preferential wetting of fluid along the wall, and e) polymerization; the final synthesized particle elongated to preserve the initial volume. B) sequence B; a) loading of wetting solution (*n*-hexadecane), b) removal of excess wetting solution by tilting, c) generation of interface between hexadecane and air, d) pouring of PEG-DA solution onto the PDMS mold and overflow of hexadecane along the PDMS wall because of the difference in densities, e) removal of excess solutions of PEG-DA and wetting solution, and f) polymerization. *d* diameter of curvature, F_d downward pressure driving force, F_u upward capillary force along the PDMS wall, w_p width of the microwell.

air/PEG-DA, respectively. Although identical micromolds were used in both processes, the difference in interfacial properties resulted in particles with different curvatures and aspect ratios. Also, PDMS molds with various shapes of microwell arrays on its surface were used.

The photocurable solution in each microwell was selectively polymerized under UV light to leave the wetting solution (*n*-hexadecane) on the hydrophobic mold. This step resulted in the generation of polymeric particles with the shape of the microwell. It is possible to control the curvature of the top and the aspect ratio with the following critical factors: 1) the capillary action of the wetting solution and formation of interfaces induced by the sequence in the procedure (sequences A and B), 2) the difference in densities between the photocurable solution and the wetting solution, and 3) the aspect ratio of the mold (height/width). In the case of sequence A, the particle curvature is formed by the evolution of the interface between the two fluids, PEG-DA and *n*-hexadecane. The interface shape depends on the interfacial tension between PEG-DA, *n*-hexadecane, and the wall of the PDMS micromold (W; Figure 1 A). Firstly, PEG-DA was loaded in the PDMS mold and the excess solution was removed (Figure 1 A, a–c). The PEG-DA solution has a contact angle θ after the wetting solution (*n*-hexadecane) was added (Figure 1 A, d, e).

The hydrophobic property of hexadecane promoted higher wettability on the PDMS side wall than the relatively hydrophilic PEG-DA. The wetting solution on the PDMS side wall induced a capillary force on the mold surface with contact angle Φ. This force generated a significant work of adhesion and, consequently, the hexadecane solution moved downwards to the bottom of the PDMS micromold. Simultaneously, the PEG-DA solution in the microwell was separated from the surface of the PDMS microwell because of lower wettability on the hydrophobic PDMS wall. Eventually, this separation resulted in the reduction of the width of PEG-DA solution in the well, thus increasing the height of the PEG-DA solution to conserve the initial volume of PEG-DA. Once elongated, the top of the PEG-DA solution produced an interface contacting the wetting solution. Finally, to minimize energy, the shape of the top became convex.

The driving force for the formation of flat-top particles (sequence B) was different from sequence A (Figure 1 B). Sequence B started with the loading of a well with wetting solution, followed by the introduction of the solution of PEG-DA. The solution of *n*-hexadecane preferentially wetted the hydrophobic PDMS mold, to result in a contact angle of hexadecane on PDMS (ψ; Figure 1 B, a–c). The solution of PEG-DA was then introduced onto the top of the *n*-hexadecane solution in a well. The larger density of PEG-DA pushed the *n*-hexadecane solution away from the well (PEG-DA $= 1.12\ g\,mL^{-1}$, *n*-hexadecane $= 0.77\ g\,mL^{-1}$). The excess solution was carefully discarded and photo-polymerizaton was initiated by UV irradiation to produce flat-top particles (Figure 1 B, d, e).

Typical examples of results of these two routes are shown in Figure 2. The SEM image of arrays of synthetic microparticles in a PDMS micromold with cylindrical wells (40 μm in radius, 59 μm in depth) confirms that our proposed method controls the convexity of particles and enables formation of anisotropic particles (bullet shapes) in a high-throughput manner (Figure 2 A).

The use of a cylindrical microwell that forms flat-top cylinder structures along the air/PEG-DA interface, with the wetting fluid on the wall of the microwell, is shown in Figure 2 B. After the release of particles from the micromold by bending the mold, SEM images confirmed the different morphologies and dimensions of the particles produced, even though identical micromolds were used (Figure 2 C, D). It is important to note that the use of sequence A produces microparticles that have a curvature at the top, a larger height, and a smaller width because of the shrinkage of the PEG-DA solution along the direction of the width. The shrinkage is driven by the capillarity of the wetting solution before photopolymerization (Figure 2 A,C). Therefore, we

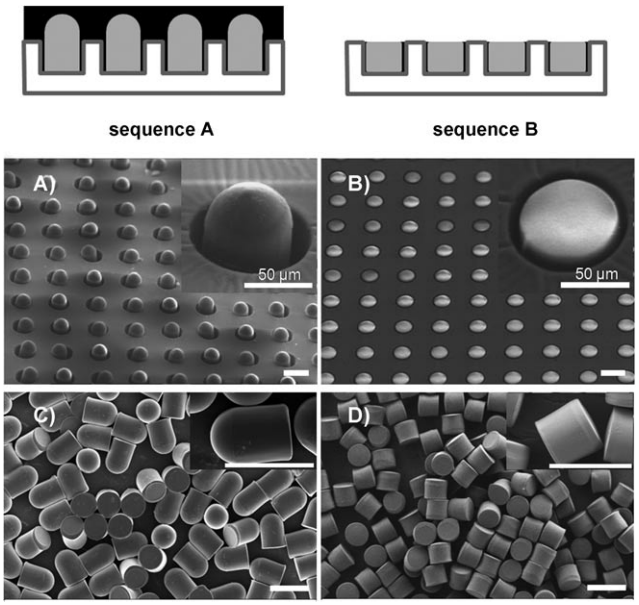

Figure 2. SEM images of particles produced by following the two sequences. The array format of A) concave cylindrical particles (bullet shapes) formed using sequence A, and B) flat-top particles using sequence B. C, D) Images recorded after the detachment of fabricated particles from the PDMS mold. The bullet-shaped particles were produced by using sequence A. Cylindrical particles were obtained by following sequence B. All of the inset SEM images clearly indicate single polymerized microparticles at each step. Scale bar in C and D: 100 μm.

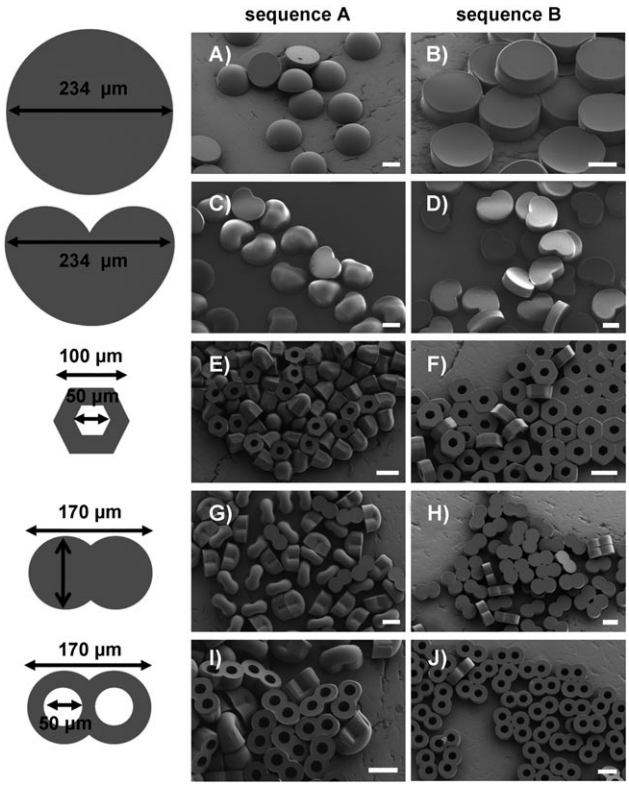

Figure 3. Fabrication of various complex particles using two procedures: curved microparticles (A, C, E, G, and I) were formed by following sequence A. The other particles were obtained by following sequence B, which, as expected, always produced anisotropic particles with flat-top structures (B, D, F, H, and J). All of the particles were synthesized by following sequences A and B. Scale bars: 100 μm.

confirm that the proposed method can control the anisotropic 3D shapes of particles by using two different methods.

In principle, we can change the pattern of the original mask to obtain particles of any shape and depth. As a proof of concept, we investigated the formation of particles by various types of molds. The capabilities of our method for the fabrication of various types of monodisperse microparticles with controlled shapes and dimensions are shown in Figure 3. The size and shape of the microparticles can also be determined by the aspect ratio of the PDMS micromold. In contrast to the results shown in Figure 2, we obtained hemispheres (from sequence A) and disk-shaped particles (from sequence B) when cylindrical micromolds that were similar but with lower aspect ratios were used (Figure 3 A, B). In addition, we fabricated various shapes such as hearts (Figure 3 C, D), hexagons (Figure 3 E,F), twin cylinders (Figure 3 G, H), and fused twin donuts (Figure 3 I, J). All the particles exhibit good fidelity to the features of the mold.

The flat-topped particles (sequence B) can be synthesized using the PRINT method, but the curved-top anisotropic particles (sequence A) are not easy to produce with PRINT because it uses nonwetting molds without wetting fluids. To make curved-top particles using PRINT, the printing micromold should have curvature, which is difficult to achieve with soft lithography. The particles obtained by using sequence B have straight and flat tops (Figure 3 B, D, F, H, J). A distinct advantage of the method proposed is the fabrication of particles that have one closed end (Figure 3 E, I). The holes in the particles did not penetrate through them by making a curved top in contrast to a flat top (Figure 3 F, J). To the best of our knowledge, no other methods can be used to selectively close a the ends of single particles.

The combination of sequences A and B is also promising for the fabrication of Janus particles. To clearly visualize each compartment of Janus particles obtained from different combinations of sequences A and B, the fluorescent dyes Rhodamine and fluorescein isothiocyanate (FITC) were loaded into solutions of trimethylolpropane triacrylate (TMPTA; another photocurable solution) and PEG-DA, respectively, in order to fabricate a model system (Figure 4). Figure 4 A shows the formation of concave-flat Janus particles using a combination of sequences A and B. Similarly, the sequential combination of sequence B with the second stage of sequence B created a flat-flat architecture in a plane parallel to the bottom of microwell (Figure 4 B). Although the morphology of the two compartments of the anisotropic Janus particles was identical, we modulated the chemical composition of each compartment to control the ratio between them. As the reverse case of Figure 4 A, the flat-concave Janus particles having a flat interface were fabricated from the combination of sequences B then A (Figure 4 C).

The Janus particles clearly show the concavity of TMPTA in the upper part and the rectangle of PEG-DA in the lower part. All Janus particles show that the fluorescent dyes were homogeneously distributed in their respective compartments,

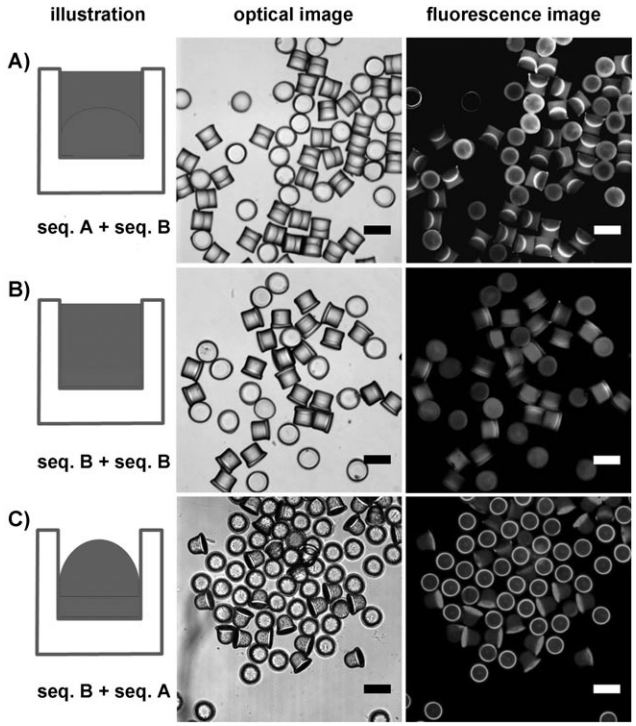

Figure 4. Generation of anisotropic Janus particles. The volume of the compartment can be also altered by the changing the volume of each of the polymerizing fluids (TMPTA and PEG-DA). A) Concave-flat Janus particles, B) flat-flat Janus particles, and C) flat-concave Janus particles. Scale bars = 100 μm.

suggesting that the compartment can be applied to cargo for encapsulating agents and the chemical functionality of each compartment can be modulated. This result confirms the utility of our approach for synthesis of novel anisotropic Janus particles that have segregated chemical or physical properties, with the capability of independent functionalization of each compartment.

In conclusion, we have presented a convenient approach for the generation of microparticles by controlling the interfacial properties and wetting of the fluids. The interfacial properties, aspect ratio of the microwells, and the process sequence chosen were used to finely tune the 3D morphology of the particles. Our method has the following advantages: 1) we can control the 3D shape of the particles by synthesizing two different particles with one mold; 2) we can manipulate the curvature of particles; 3) it is possible to make an ordered array of particles, which can be directly used in high throughput screening; 4) the process can be parallelized to increase the production rate; and 5) it is possible to make particles with multiple components without additional control devices.

This proposed methodology for the synthesis of anisotropic particles can be applied for novel material synthesis in wide variety of applications such as photonics, liquid crystals, and optics. Particles with different curvatures can be used to mimic the wealth of microscale shapes found in nature such as bacteria, platelets, or erythrocytes. The particles can also be used in new applications in advanced materials, which take advantage of their unique scattering properties as well as precise control over shape and size.

Received: May 7, 2010
Published online: September 2, 2010

Keywords: interfaces · micromolding · microparticles · polymerization · surface tension

[1] H. Y. He, X. Cao, L. J. Lee, *J. Controlled Release* **2004**, *95*, 391.
[2] A. K. Andrianov, L. G. Payne, *Adv. Drug Delivery Rev.* **1998**, *34*, 155.
[3] W. R. Gombotz, S. F. Wee, *Adv. Drug Delivery Rev.* **1998**, *31*, 267.
[4] C. H. J. Schmitz, A. C. Rowat, S. Koster, D. A. Weitz, *Lab Chip* **2009**, *9*, 44.
[5] S. L. Tao, T. A. Desai, *Adv. Mater.* **2005**, *17*, 1625.
[6] S. E. A. Gratton, P. D. PohhauS, J. Lee, I. Guo, M. J. Cho, J. M. DeSimone, *J. Controlled Release* **2007**, *121*, 10.
[7] J. W. Kirnt, A. Fernandez-Nieves, N. Dan, A. S. Utada, M. Marquez, D. A. Weitz, *Nano Lett.* **2007**, *7*, 2876.
[8] R. A. Petros, P. A. Ropp, J. M. DeSimone, *J. Am. Chem. Soc.* **2008**, *130*, 5008.
[9] B. Laulicht, P. Cheifetz, E. Mathiowitz, A. Tripathi, *Langmuir* **2008**, *24*, 9717.
[10] M. C. W. van Boxtel, R. H. C. Janssen, D. J. Broer, H. T. A. Wilderbeek, C. W. M. Bastiaansen, *Adv. Mater.* **2000**, *12*, 753.
[11] R. P. Kulkarni, D. D. Wu, M. E. Davis, S. E. Fraser, *Proc. Natl. Acad. Sci. USA* **2005**, *102*, 7523.
[12] G. S. Chirica, V. T. Remcho, *Anal. Chem.* **2000**, *72*, 3605.
[13] a) S. E. A. Gratton, P. A. Ropp, P. D. Pohlhaus, J. C. Luft, V. J. Madden, M. E. Napier, J. M. DeSimone, *Proc. Natl. Acad. Sci. USA* **2008**, *105*, 11613; b) H. Zhang, J. K. Nunes, S. E. A. Gratton, K. P. Herlihy, P. D. Pohlhaus, J. M. DeSimone, *New J. Phys.* **2009**, *11*, 0.
[14] J. A. Champion, S. Mitragotri, *Proc. Natl. Acad. Sci. USA* **2006**, *103*, 4930.
[15] M. Singh, C. P. Morris, R. J. Ellis, M. S. Detamore, C. Berkland, *Tissue Eng. Part C* **2008**, *14*, 299.
[16] L. Alexander, K. Dhaliwal, J. Simpson, M. Bradley, *Chem. Commun.* **2008**, 3507.
[17] M. Bradley, J. Rowe, *Soft Matter* **2009**, *5*, 3114.
[18] A. Perro, S. Reculusa, S. Ravaine, E. B. Bourgeat-Lami, E. Duguet, *J. Mater. Chem.* **2005**, *15*, 3745.
[19] P. Akcora, H. Liu, S. K. Kumar, J. Moll, Y. Li, B. C. Benicewicz, L. S. Schadler, D. Acehan, A. Z. Panagiotopoulos, V. Pryamitsyn, V. Ganesan, J. Ilavsky, P. Thiyagarajan, R. H. Colby, J. F. Douglas, *Nat. Mater.* **2009**, *8*, 354.
[20] H. A. Jerri, R. A. Dutter, D. Velegol, *Soft Matter* **2009**, *5*, 827.
[21] D. Dendukuri, P. S. Doyle, *Adv. Mater.* **2009**, *21*, 4071.
[22] N. Prasad, J. Perumal, C. H. Choi, C. S. Lee, D. P. Kim, *Adv. Funct. Mater.* **2009**, *19*, 1656.
[23] D. Dendukuri, T. A. Hatton, P. S. Doyle, *Langmuir* **2007**, *23*, 4669.
[24] V. Palermo, P. Samori, *Angew. Chem.* **2007**, *119*, 4510; *Angew. Chem. Int. Ed.* **2007**, *46*, 4428.
[25] T. Deng, H. K. Wu, S. T. Brittain, G. M. Whitesides, *Anal. Chem.* **2000**, *72*, 3176.
[26] J. J. Guan, H. Y. He, L. J. Lee, D. J. Hansford, *Small* **2007**, *3*, 412.
[27] S. Badaire, C. Cottin-Bizonne, J. W. Woody, A. Yang, A. D. Stroock, *J. Am. Chem. Soc.* **2007**, *129*, 40.
[28] C. J. Hernandez, T. G. Mason, *J. Phys. Chem. C* **2007**, *111*, 4477.
[29] J. A. Champion, Y. K. Katare, S. Mitragotri, *Proc. Natl. Acad. Sci. USA* **2007**, *104*, 11901.

[30] A. C. Courbaron, O. J. Cayre, V. N. Paunov, *Chem. Commun.* **2007**, 628.
[31] C. H. Choi, J. H. Jung, D. W. Kim, Y. M. Chung, C. S. Lee, *Lab Chip* **2008**, *8*, 1544.
[32] S. E. Chung, W. Park, S. Shin, S. A. Lee, S. Kwon, *Nat. Mater.* **2008**, *7*, 581.
[33] D. Dendukuri, D. C. Pregibon, J. Collins, T. A. Hatton, P. S. Doyle, *Nat. Mater.* **2006**, *5*, 365.
[34] J. Wan, A. Bick, M. Sullivan, H. A. Stone, *Adv. Mater.* **2008**, *20*, 3314.
[35] C. H. Chen, A. R. Abate, D. Y. Lee, E. M. Terentjev, D. A. Weitz, *Adv. Mater.* **2009**, *21*, 3201.
[36] W. Li, H. H. Pharn, Z. Nie, B. MacDonald, A. Guenther, E. Kumacheva, *J. Am. Chem. Soc.* **2008**, *130*, 9935.
[37] J. I. Park, Z. Nie, A. Kumachev, A. I. Abdelrahman, B. R. Binks, H. A. Stone, E. Kumacheva, *Angew. Chem.* **2009**, *121*, 5404; *Angew. Chem. Int. Ed.* **2009**, *48*, 5300.
[38] S. Xu, Z. Nie, M. Seo, P. Lewis, E. Kumacheva, H. A. Stone, P. Garstecki, D. B. Weibel, I. Gitlin, G. M. Whitesides, *Angew. Chem.* **2005**, *117*, 3865; *Angew. Chem. Int. Ed.* **2005**, *44*, 3799.
[39] J. P. Rolland, B. W. Maynor, L. E. Euliss, A. E. Exner, G. M. Denison, J. M. DeSimone, *J. Am. Chem. Soc.* **2005**, *127*, 10096.
[40] D. C. Duffy, J. C. McDonald, O. J. A. Schueller, G. M. Whitesides, *Anal. Chem.* **1998**, *70*, 4974.

